Developmental Biology 452 (2019) 134–143

Contents lists available at ScienceDirect

Developmental Biology

journal homepage: www.elsevier.com/locate/developmentalbiology

Isl1-expressing non-venous cell lineage contributes to cardiac lymphatic vessel development

Kazuaki Maruyama [a], Sachiko Miyagawa-Tomita [a,b,c], Kaoru Mizukami [a], Fumio Matsuzaki [d], Hiroki Kurihara [a,e,*]

[a] Department of Physiological Chemistry and Metabolism, Graduate School of Medicine, The University of Tokyo, 7-3-1 Hongo, Bunkyo-ku, Tokyo, 113-0033, Japan
[b] Department of Pediatric Cardiology, Tokyo Women's Medical University, 8-1 Kawada-cho, Shinjuku-ku, Tokyo, 162-8666, Japan
[c] Department of Animal Nursing Science, Yamazaki University of Animal Health Technology, 4-7-2 Minami-osawa, Hachioji, Tokyo, 192-0364, Japan
[d] Laboratory for Cell Asymmetry, RIKEN Center for Developmental Biology, 2-2-3, Minatojiima-Minamimachi, Chuou-ku, Kobe, 650-0047, Japan
[e] Core Research for Evolutional Science and Technology (CREST), Japan Science and Technology Agency (JST), Chiyoda-ku, Tokyo, 102-0076, Japan

A B S T R A C T

The origin of the mammalian lymphatic vasculature has been studied for more than a century; however, details regarding organ-specific lymphatic development remain unknown. A recent study reported that cardiac lymphatic endothelial cells (LECs) stem from venous and non-venous origins in mice. Here, we identified *Isl1*-expressing progenitors as a potential non-venous origin of cardiac LECs. Genetic lineage tracing with *Isl1-Cre* reporter mice suggested a possible contribution from the *Isl1*-expressing pharyngeal mesoderm constituting the second heart field to lymphatic vessels around the cardiac outflow tract as well as to those in the facial skin and the lymph sac. Isl1^{+} lineage-specific deletion of Prox1 resulted in disrupted LYVE1^{+} vessel structures, indicating a Prox1-dependent mechanism in this contribution. Tracing back to earlier embryonic stages revealed the presence of VEGFR3^{+} and/or Prox1^{+} cells that overlapped with the Isl1^{+} pharyngeal core mesoderm. These data may provide insights into the developmental basis of heart diseases involving lymphatic vasculature and improve our understanding of organ-based lymphangiogenesis.

1. Introduction

The lymphatic vasculature is a major component of the systemic circulatory system, maintaining tissue fluid homeostasis by draining the interstitial fluid (lymph) into the bloodstream. It also plays important roles in inflammation, the immune response, and lipid absorption from the gut, and is also known to be a major route for tumor metastasis (Oliver and Alitalo, 2005). The origin of lymphatic vessels has long been a subject of controversy since the early 1900s, when a model was formulated in which the initial lymph sacs originate by budding from venous endothelial cells (ECs), before spreading into the systemic lymphatic system (Sabin, 1902). Another model proposed that lymph sacs arise from the mesenchyme and connect to veins (Huntington and McClure, 1910). Nowadays, the former model is widely accepted. However, little is known about organ-specific lymphatic development, and investigations on this topic are still at an early stage.

In mice, lymphatic vessels arise from the anterior cardinal vein between embryonic day (E) 9.5 and E10.0, when a part of endothelial cells in the cardinal vein become committed to the lymphatic fate by expressing prospero homeobox transcription protein 1 (Prox1) (Srinivasan et al., 2007; Wigle and Oliver, 1999). After E10.0, vascular endothelial growth factor C (VEGF-C) induces paracrinally the sprouting of VEGFR3-positive lymphatic endothelial cells (LECs) from the cardinal vein to form the first lymphatic plexus (Hägerling et al., 2013; Karkkainen et al., 2004). This venous contribution was validated in zebrafish (Koltowska et al., 2015; Nicenboim et al., 2015). By contrast, in frogs and birds, additional sources of LECs contribute to lymphatic vessel formation during development (Ny et al., 2005; Schneider et al., 1999; Wilting et al., 2006). Recent works performed in mouse models have revealed that non-venous sources of LECs also contribute to lymphatic vasculature in the skin, mesentery and heart (Klotz et al., 2015; Martinez-Corral et al., 2015; Stanczuk et al., 2015).

The heart carries an extensive lymphatic vasculature, the physiological role of which has long been an enigma (Johnson and Blake, 1966; Shore, 1929). Recent reports have revealed that, in pathological conditions such as myocardial infarction, cardiac lymphatic vessels regulate tissue fluid balance and immune reactions of the injured heart, while stimulation of lymphangiogenesis with VEGF-C can improve cardiac function following myocardial injury, leaving a reduced fibrotic area (Henri et al., 2016; Klotz et al., 2015). Although the developmental

* Corresponding author. Department of Physiological Chemistry and Metabolism, Graduate School of Medicine, The University of Tokyo, 7-3-1 Hongo, Bunkyo-ku, Tokyo, 113-0033, Japan.
E-mail address: kuri-tky@umin.net (H. Kurihara).

https://doi.org/10.1016/j.ydbio.2019.05.002
Received 16 March 2018; Received in revised form 1 May 2019; Accepted 2 May 2019
Available online 18 May 2019

origins of cardiac LECs has been unclear, a recent study proposed that sprouts from the venous endothelium are the primary source of LECs, whereas hemogenic endothelial cells serve as a non-venous source of LECs during embryonic lymphangiogenesis (Klotz et al., 2015).

In this study, we have identified *Isl1*-expressing progenitors as another non-venous origin of cardiac LECs during mouse development. Genetic lineage tracing and conditional knockout of *Prox1* using *Isl1-Cre* mice indicate that *Isl1*-expressing mesodermal cells in the pharyngeal region serve as a potential source of LECs, which contributes to cardiac lymphatic vessel formation. The *Isl1*-expressing pharyngeal mesoderm

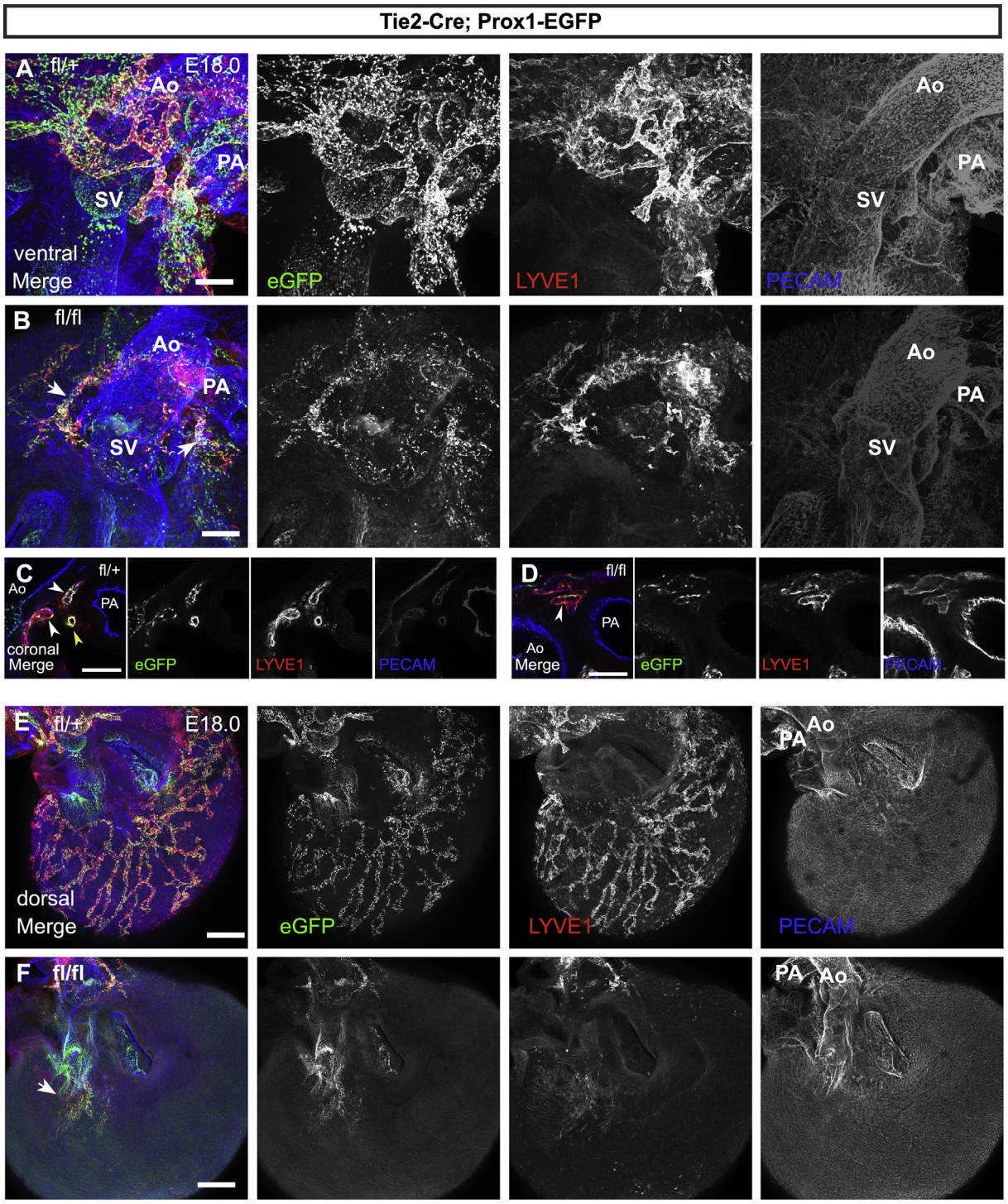

Fig. 1. Inactivation of Prox1 in the Tie2^{+} lineage results in impaired lymphatic vessel formation with regional differences. Confocal images of hearts labeled for PECAM, eGFP, and LYVE1 at E18.0 **(A, B, E, F).** Many eGFP^{+} cells expressing Prox1 co-express PECAM and LYVE1, forming lymphatic vessels on the ventral (**A**) and dorsal (**E**) sides of Tie2-Cre; Prox1$^{fl/+}$ hearts at E18.0. Tie2-Cre; Prox1$^{fl/fl}$ hearts show a decreased number of eGFP^{+} LECs around the aorta (**B**, white arrows) and scarce lymphatic vessels on the dorsal ventricular wall (**F**, white arrow). Cardiac lymphatic vessels on the dorsal side of the aorta in Tie2-Cre; Prox1$^{fl/+}$ hearts (**C**) and Tie2-Cre; Prox1$^{fl/fl}$ hearts (**D**). In Tie2-Cre; Prox1$^{fl/+}$ hearts, both eGFP^{-} (white arrowheads) and eGFP^{+} (yellow arrowhead) LECs are detected. By contrast, the remaining LECs are mostly negative for eGFP in Tie2-Cre; Prox1$^{fl/fl}$ hearts (white arrowhead). Ao, aorta; PA, pulmonary artery; SV, sinus of Valsalva. Scale bars, 100 μm **(A-D)**, 500 μm **(E, F)**.

constitutes a multipotent cell population named the second heart field (SHF), which gives rise to cardiac components including cardiomyocytes in the right ventricle and both atria, smooth muscle cells of the great vessels, and vascular endothelial cells. Thus, a subpopulation of cardiac LECs may share a common origin with various cardiac components. Our results may provide an insight into the understanding of the stepwise process of cardiac lymphatic vessel formation and the fundamental basis for lymphangiogenesis-related diseases. This may lead to future therapeutic interventions to cardiac injury through lymphangiogenic mechanisms.

2. Results

2.1. Regional differences in venous and non-venous contributions to cardiac lymphatic vessel formation

To investigate the origins of cardiac LECs and their regional contribution, we crossed *Prox1* conditional knockout (KO) mice, which express eGFP under the control of the *Prox1* promoter upon Cre-mediated exon 2 deletion (Iwano et al., 2012), with different Cre-expressing mice. Crossing with *Tie2-Cre* mice, which express Cre in vascular endothelial cells, resulted in extensive eGFP labeling of cardiac lymphatic vessels marked by LYVE1 staining in the *Tie2-Cre;Prox1*$^{fl/+}$ heterozygous state (Fig. 1A, E), as previously reported by Klotz et al(Klotz et al., 2015). The *Tie2-Cre;Prox1*$^{fl/fl}$ homozygous state lead to an ectopic surface vasculature with bleeding at E15.5 and E17.5 (Supplemental Fig. 1A-C) and hypoplastic cardiac lymphatic vessels (Fig. 1B, F), confirming the findings of the previous report by Klotz et al. Notably, the severity of the cardiac lymphatic phenotype of *Tie2-Cre;Prox1*$^{fl/fl}$ mice demonstrated a regional difference. While there were very few cardiac LYVE1$^+$ LECs on the dorsal side (Fig. 1E, F), the number of LYVE1$^+$ LECs was relatively preserved on the lateral and ventral side of the outflow region, although they did not appear to form a vascular network efficiently (Fig. 1A, B). Some LYVE1$^+$ LECs on the right lateral side were positive for eGFP (Supplemental Fig. 1D), but many other LYVE1$^+$ LECs in the ventral outflow region of *Tie2-Cre;Prox1*$^{fl/fl}$ were largely negative for eGFP (Fig. 1A–D), indicating that cells of non-venous origin contribute to lymphatic vessel formation. Instead, aberrant LYVE1-negative microvasculature was formed by eGFP$^+$/PECAM$^+$ cells around the aortic stem sites (Supplemental Fig. 1E, F).

To confirm the phenotypic regional difference, we then statistically analyzed eGFP$^+$ area in LYVE1$^+$ lymphatic vessels. In the dorsal side, LYVE1$^+$ area was decreased in *Tie2-Cre;Prox1*$^{fl/fl}$ mice. In the outflow region around the aorta, LYVE1$^+$ area was also decreased in *Tie2-Cre;Prox1*$^{fl/fl}$ mice (Supplemental Fig. 1G). In the LYVE1$^+$ vascular area in this region, the eGFP$^+$ compartment was significantly decreased, whereas the eGFP$^-$ compartment was preserved (Supplemental Fig. 1H-K). These results suggest that the contribution of the Tie2$^-$ non-venous lineage(s) is relatively high in LECs in the outflow region, although LECs of Tie2$^+$ venous origin are necessary for the formation of an intact vascular network in this region.

2.2. Isl1-expressing progenitors in the pharyngeal region serve as a source of LECs

Klotz et al. have revealed that the Vav1$^+$ hemogenic lineage contributes to cardiac LECs as a non-venous origin. On the other hand, cardiac structures of the outflow tract region are highly contributed to by the SHF, a progenitor population in the pharyngeal region with multidirectional differentiation potential. We then speculated that the SHF might serve as another non-venous origin of cardiac lymphatic vessels. To investigate this possibility, we first used *Isl1-Cre;R26R-eYFP* mice, in which SHF-derivatives are labeled with eYFP. Immunohistochemical analysis of eYFP, the endothelial marker PECAM and the early LEC marker Prox1 revealed that a number of Prox1$^+$/PECAM$^-$ cells in the pharyngeal arches were positive for eYFP at E11.5 (Fig. 2A, B; 22.8 ± 2.3%, eGFP$^+$/Prox1$^+$ cells (n = 3)), whereas Prox1$^+$ cells in the common cardinal veins were not (Fig. 2C). At E13.5, a population of Prox1$^+$ and PECAM^{+-} cells were distributed continuously in the aortic wall, expressing eYFP together with surrounding aortic mural cells (Fig. 2D, E; 54.2 ± 8.2%, eGFP$^+$/Prox1$^+$ cells (n = 4)). Prox1$^+$/eYFP$^+$ LECs were also detected in the jugular lymph sac (Supplemental Fig. 2A-C; 8.2 ± 2.3%, eGFP$^+$/Prox1$^+$ cells (n = 4), whereas no Prox1$^+$/eYFP$^+$ LECs were found in the jugular vein (Supplemental Fig. 2C). Lymphatic vessels around the outflow tract and ventral side of the ventricles were also positive for PECAM, Prox1, and eYFP at E17.5 (Fig. 2F, G; 24.2 ± 2.2%, eGFP$^+$/Prox1$^+$ cells (n = 4)). To further confirm the contribution of *Isl1*-expressing progenitors to cardiac lymphatic vessels, we performed immunostaining for eGFP, Prox1 and LYVE1 at E17.5. We confirmed eGFP$^+$/Prox1$^+$/LYVE1$^+$ lymphatic vessels on the outflow

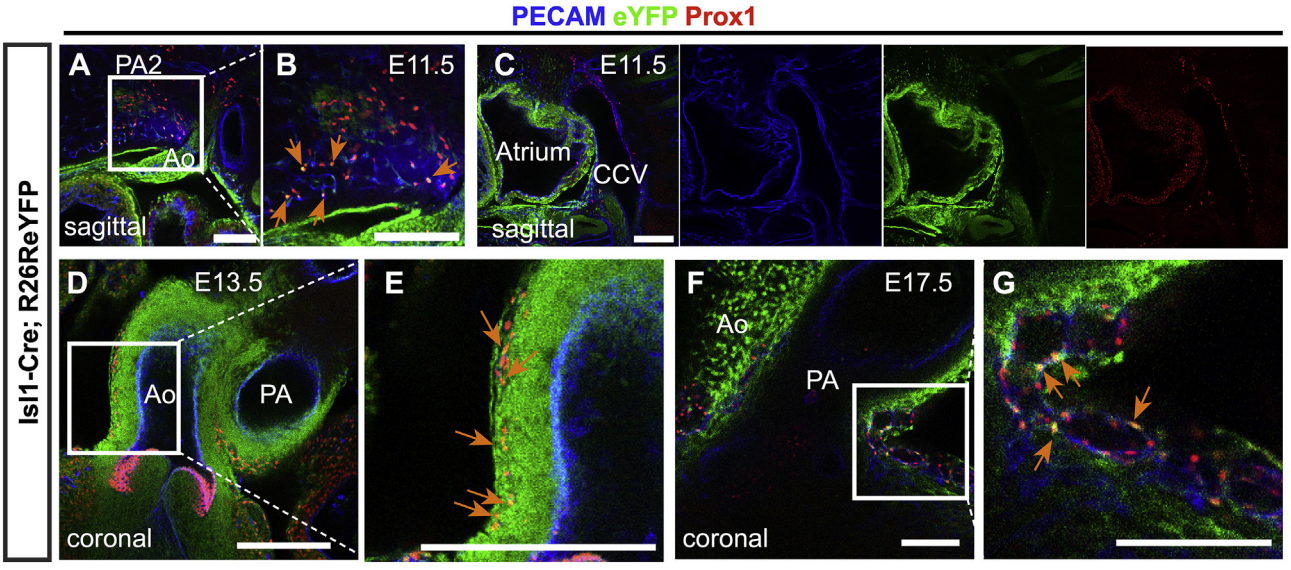

Fig. 2. The Isl1$^+$ lineage contributes to cardiac lymphatic vessels. **(A-I)** Confocal imaging of Isl1-Cre; R26ReYFP labeled for PECAM, eYFP, and Prox1 at E11.5, E13.5, and E17.5. **(A, B)** eYFP is colocalized with Prox1 in the second PA (orange arrows). **(C)** eYFP is not colocalized with Prox1 in the CCV endothelium (n = 3). **(D, E)** eYFP is colocalized with Prox1 around the aorta at E13.5 (orange arrows). **(F, G)** eYFP is colocalized with Prox1 around the outflow tract at E17.5 (orange arrows). PA2, second pharyngeal arch; Ao, aorta; CCV, common cardinal vein; PA pulmonary artery. Scale bars, 100 μm **(A-C),** 50 μm **(D-G)**.

tract region (Supplemental Fig. 3A-C), whereas lymphatic vessels on the dorsal side of the ventricles were not (Supplemental Fig. 3D, E). Thus, cardiac lymphatic vessels are likely to develop from two different origins, the cardinal vein and *Isl1*-expressing non-venous progenitors, except on the dorsal side of the heart. Taken together with a previous report that initial cardiac lymphatic vessels first emerge around the aorta (described as extra-cardiac regions) at E12.5 (Klotz et al., 2015), Prox1$^+$ cells may arise from the SHF in the region spanning the pharyngeal arches and the cardiac outflow tract, and contribute to cardiac lymphatic vessel formation via the immature vascular plexus in cooperation with venous-derived LECs.

Lineage-specific *Prox1* knockdown reveals the contribution of the second heart field to lymphatic vessel formation.

To further analyze the possible contribution of SHF-derived Prox1$^+$ cells to cardiac lymphatic vessel formation, we crossed *Prox1* conditional KO mice with *Isl1-Cre* mice. Resultant *Isl1-Cre;Prox1$^{fl/fl}$* mice exhibited Cre-dependent eGFP expression representing Isl1$^+$ lineage distribution. The eGFP expression was observed in the SHF-derived facial tissues, cardiac outflow regions and the right ventricle at E17.5 (Supplemental Fig. 4A-D). The *Isl1-Cre;Prox1$^{fl/fl}$* homozygous state lead to a subcutaneous bleeding restricted to the facial region at E17.5 (Supplemental Fig. 4E, F). Correspondingly, eGFP$^+$ cells contributed to LECs in the facial skin (Supplemental Fig. 4G, H).

In *Isl1-Cre;Prox1$^{fl/+}$* mice, the eGFP$^+$ lineage contributed to lymphatic vessels around the aorta and on the ventral side of the heart, but did not contribute to those on the dorsal side of the heart (Fig. 3A–D, I, J). In *Isl1-Cre;Prox1$^{fl/fl}$* homozygous mice, LYVE1$^+$ lymphatic vessel formation was impaired particularly on the ventral side of the heart (Fig. 3E–H). On the ventral side of the outflow tract in homozygous mice, LYVE1$^+$ cells were decreased and did not apparently form mature thick vessels (Fig. 3K-M). Quantitative analysis showed that lymphatic vessels in the outflow region were composed of Isl1$^+$ and Isl1$^-$ components, both of which were decreased in homozygous mutants (Fig. 3N–Q). These results suggest that Prox1$^+$ cells derived from the Isl1$^+$ lineage contribute to the formation of cardiac lymphatic vessels around the aorta and the ventral side of the ventricles through cell-autonomous and non-autonomous mechanisms. On the dorsal side of the heart, lymphatic vessels also appeared to be underdeveloped, although to a lesser extent (Fig. 3C, G). In addition to the lymphatic lineage, Prox1-driven eGFP expression was broadly observed in the right ventricle and outflow tract cardiomyocytes as reported previously (Risebro et al., 2009). *Isl1-Cre;Prox1$^{fl/fl}$* homozygous mice had apparently smaller hearts compared to the control hearts, as in the case with cardiomyocyte-specific Prox1 deletion (Risebro et al., 2009), but showed neither major abnormalities such as ventricular septal defect (Supplemental Fig. 4I) nor prenatal lethality (n = 7 and 6 for *Isl1-Cre;Prox1$^{fl/+}$* and *Isl1-Cre;Prox1$^{fl/fl}$* mice, respectively).

2.3. Spatiotemporal analysis of Isl1$^+$ lineage-derived LEC development

To further explore possible progenitors of cardiac LECs in the SHF, we performed immunohistochemical analysis of endothelial marker expression in embryos at early developmental stages. Prox1 expression was detected in a portion of the common cardinal vein at E9.5 and E10.5, expanding to the dorsal side at E10.5 (Fig. 4A, B, D, E), consistent with previous reports that the cardinal vein likely gives rise to a major population of LECs (Sabin, 1902; Srinivasan et al., 2007; Yang et al., 2012). In addition, Prox1$^+$ cell clusters were observed at E9.5 and E10.5 in the Isl1$^+$ core mesoderm of the first and second pharyngeal arches (Fig. 4A, C, D, F, G). At E9.5, VEGFR3$^+$/PECAM$^+$ cells are located mainly in the periphery of the Prox1$^+$ cell cluster, with partial co-expression of Prox1 (Fig. 5A, B). At E10.5, VEGFR3$^+$/PECAM$^+$ cells with and without Prox1 expression appeared to form mesh-like network structures, which extended caudally (Fig. 5C, D). At E12.5, similar mesh-like networks composed of Prox1$^+$ and/or VEGFR3$^+$ cells appeared, surrounding the outflow tract (Fig. 5E, F). At this stage, this region was mostly negative for LYVE1, whereas LYVE1$^+$ vessels were found around the sinus venosus (Fig. 6A–D). Thereafter, VEGFR3$^+$/Prox1$^+$ networks were remodeled into thick lymphatic vessels and fine mesh-like structures, and were gradually retarded around E15.0 to E16.5 (Fig. 5G–J, 6E, G). Along with this process, a LYVE1-expressing branch-like structure, seemingly a part of VEGFR3$^+$/Prox1$^+$ networks, appeared on the ventral side of the aorta at E15.0 and extended towards the ventricular surface, making connections with LYVE1$^+$ lymphatic vessels on the dorsal side around E16.5 (Fig. 6E–I). Since LYVE1 is expressed also in macrophages, we tried to confirm that branch-forming LYVE1$^+$ cells on the outflow tract were LECs rather than tissue resident macrophages by immunostaining for the macrophage marker F4/80 and LYVE1 from E14.5 to E16.5 (Supplemental Fig. 5). On the ventral side of the heart and great vessels, LYVE1$^+$ branching structures were negative for F4/80, whereas F4/80$^+$/LYVE1$^+$ cells were sporadically observed (Supplemental Fig. 5A, B, F, G, K, L). On the dorsal side, LYVE1$^+$ cells, which distributed in a scattered pattern at E14.5 and formed mesh-like networks at E15.5 and E16.5, were mostly negative for F4/80. F4/80$^+$/LYVE1$^+$ cells were mainly detected around the sinus venosus and in the epicardium at E14.5 (Supplemental Fig. 5C-E), which were decreased thereafter (Supplemental Fig. 5H-J, M-O). These results indicate that lymphangiogenic progenitors may arise in the SHF as Prox1$^+$ and/or VEGFR3$^+$ cells and contribute to cardiac lymphatic vessel formation in the outflow tract.

3. Discussion

Although extensive research has been reported on the development of systemic lymphatic vessels over the past few decades, there has been limited research focused on the establishment of organ-based lymphatics. Significant progress has been made recently in the origin of cardiac LECs, showing dual contributions by extra-cardiac venous endothelium and non-venous progenitors (Klotz et al., 2015). Using lineage-specific Cre--driver mice, hemogenic endothelium in the yolk sac has been identified as the possible non-venous origin. Here, we demonstrate that *Isl1*-expressing progenitors in the pharyngeal region serve as another non-venous origin of cardiac LECs during mouse development.

Genetic lineage tracing with *Isl1-Cre* reporter mice showed a contribution by *Isl1*-expressing progenitors to lymphatic vessels around the outflow tract and ventral side of the ventricles. In addition, we also identified their contribution to the jugular lymph sac and facial skin lymphatics, whereas it was not detected in the E11.5 common cardinal and E13.5 jugular veins. These results suggest that Isl1$^+$-progenitor-derived LECs participate in the formation of lymphatic vessel networks cooperatively with LECs of venous origin, which sprout out from the jugular vein without Isl1 labeling.

Notably, crossing *Isl1-Cre* mice with *Prox1* conditional KO mice revealed the incorporation of Isl1$^+$-progenitor-derived Prox1-expressing cells (labeled with eGFP in the heterozygous state) into LYVE1$^+$ mature lymphatic vessels, and disrupted LYVE1$^+$ vessel formation caused by the lineage-specific Prox1 deletion. This demonstrates the importance of the Isl1$^+$ lineage derivatives in cardiac lymphatic vessel formation in the outflow region via a Prox1-dependent mechanism. Notably, Isl1$^+$ lineage-specific Prox1 deletion also resulted in a decreased contribution of Isl1$^-$ cells (possibly of venous origin) to lymphatic vessel formation in this region, indicating that the Isl1$^+$ lineage might affect LECs of venous origin in a cell-nonautonomous manner.

Tracing back to earlier embryonic stages revealed the distribution of Prox1$^+$ and/or VEGFR3$^+$ cells overlapping with Isl1$^+$ cells in the pharyngeal mesodermal core. The *Isl1*-expressing pharyngeal mesoderm constitutes the anterior SHF, a multipotent progenitor population that differentiates into diverse cardiac components mainly in the outflow tract region and right ventricle. Prox1 is known to be expressed broadly in the cardiovascular system including cardiac valves and cardiomyocytes (Risebro et al., 2009). Although the early Prox1 expression in the core mesoderm may also represent such broad expression as in myogenic progenitor cells, spaciotemporal continuity between Prox1$^+$ and/or VEGFR3$^+$ cell distribution in the pharyngeal region and those in

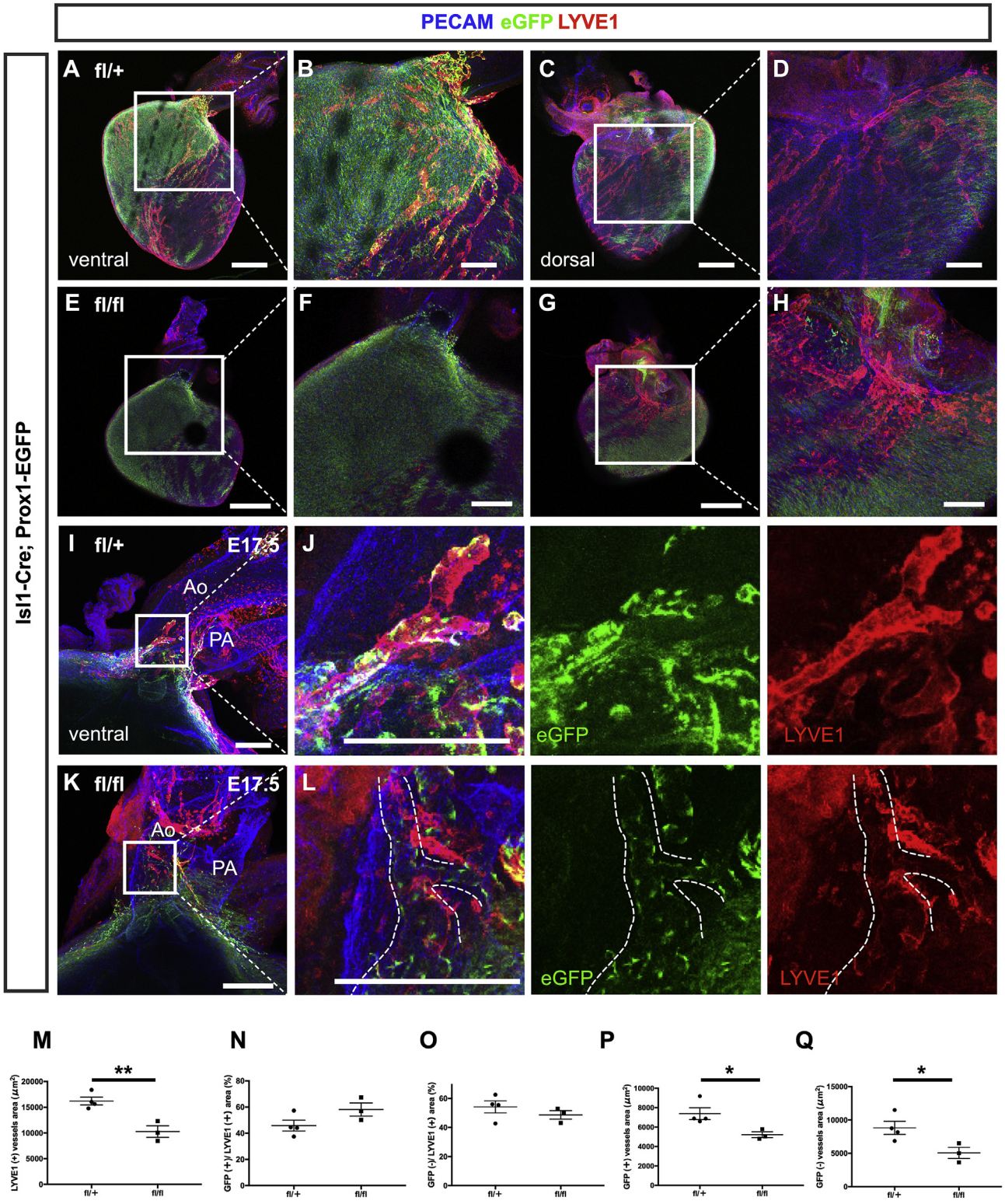

Fig. 3. Inactivation of Prox1 in the Isl1^{+} lineage reveals SHF contribution to cardiac LECs. Confocal images of hearts labeled for PECAM, eGFP and LYVE1 at E17.5. eGFP^{+} indicates cells expressing *Prox1* in Isl1-Cre; Prox1$^{fl/+}$ hearts and Isl1-Cre; Prox1$^{fl/fl}$ hearts, merged with PECAM and LYVE1. **(A-D, I, J)** In Isl1-Cre; Prox1$^{fl/+}$ embryos, eGFP expression is found in SHF-derived right ventricular cardiomyocytes (**A-D**) and LYVE1^{+} cardiac lymphatic vessels on the ventral wall (**A, B**). On the dorsal side, there was no apparent eGFP expression in lymphatic vessels (**C, D**). (**E-H, K, L**) Isl1-Cre; Prox1$^{fl/fl}$ hearts exhibit reduced eGFP^{+} lymphatic vessels around the aorta. LYVE1 staining is poorly detected in eGFP-labeled vessels in the Prox1-eGFP homozygous state (white broken lines). (**M-Q**) Quantitative analysis of lymphatic vessel formation in the outflow region. Total LYVE1^{+} area (**M**), ratios of eGFP^{+} or eGFP^{-} components of LYVE1^{+} area (**N** and **O**, respectively) and areas of each component (**P** and **Q**, respectively) in the ventral outflow tract region within 200μm above the base of the aortic valve were quantified. All the data are presented as the means ± SEM. Each dot represents a value obtained from one sample. * $P < 0.05$, ** $P < 0.01$. Ao, aorta; PA, pulmonary artery. Scale bars, 100 μm **(B, D, F, H, I, J, K, L)**, 500 μm **(A, C, E, G)**.

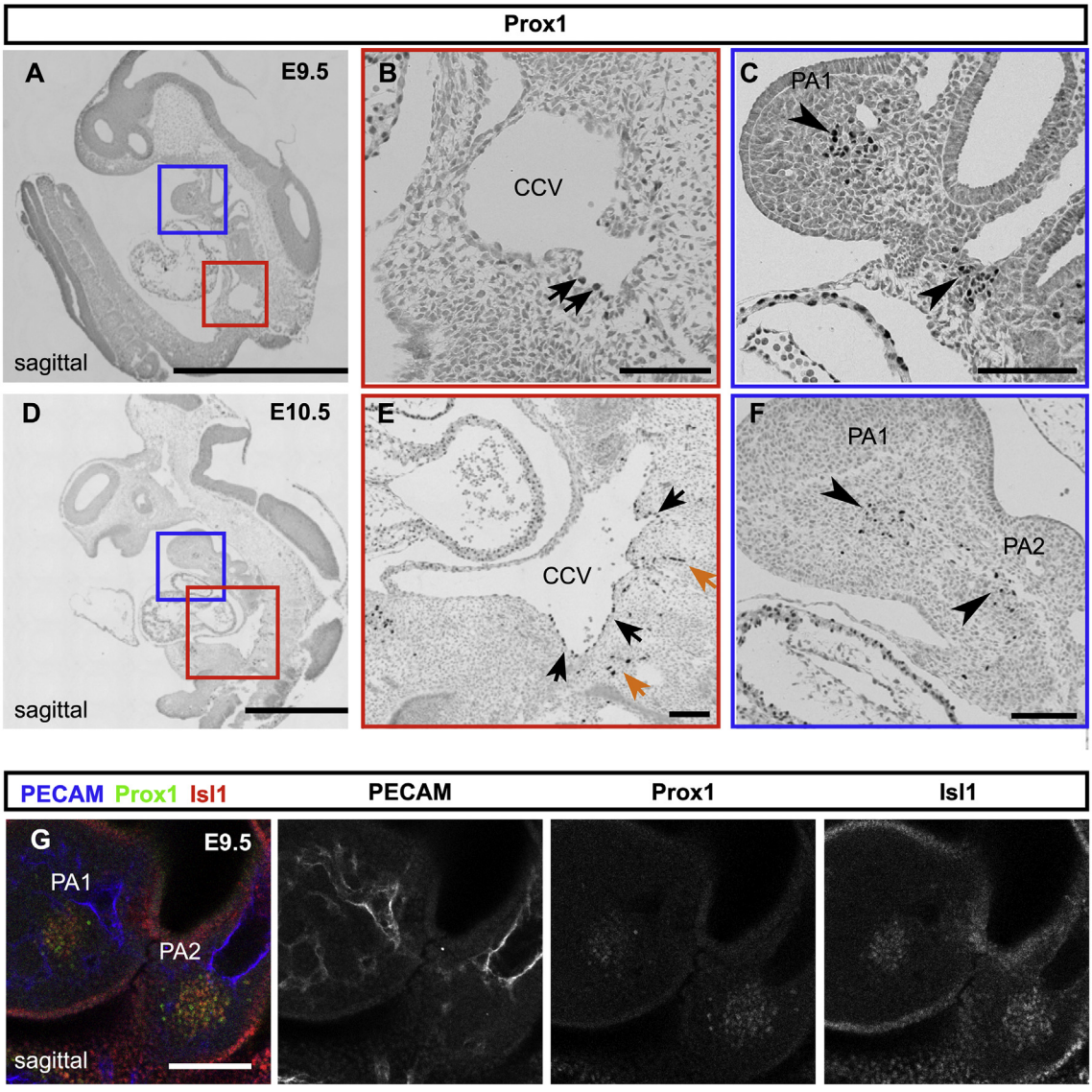

Fig. 4. Isl1^{+}/Prox1^{+} cell clusters in the pharyngeal core mesoderm. **(A-F)** Section immunohistochemistry with Prox1 labeling at E9.5 and E10.5. Boxed areas are magnified in the right panels. (**B**) A portion of the CCV expresses Prox1 at E9.5 (black arrow). (**C**) Prox1^{+} cell clusters appeared in the first and second PAs at E9.5 (black arrowheads). (**E**) Prox1-expressing CCV (black arrows) and venous-derived LECs (orange arrows) are shown in the right bottom panel. (**F**) Prox1^{+} cell clusters distribute toward the heart at E10.5 (black arrowheads). **(G)** Confocal imaging labeled for PECAM, Prox1, and Isl1 at E9.5. PECAM^{-}/Prox1^{+}/Isl1^{+} cell clusters are observed in the first and second PAs (orange arrows). PA, pharyngeal arch; CCV, common cardinal vein; LECs, lymphatic endothelial cells. Scale bars, 1 mm **(A, D)**, 100 μm **(B, C, E-G)**.

the outflow region lead us to speculate that Isl1-labeled LECs may stem from the anterior SHF and move to the outflow region together with other SHF derivatives destined to become cardiac components. Considering the key role of Prox1 in commitment and differentiation into LECs (Srinivasan et al., 2007; Wigle and Oliver, 1999), continuous Prox1 expression may switch the fate of SHF-derivatives to LEC differentiation. However, it is still possible that the effect of Prox1 on the cardiac lymphatic vessels may be indirect, considering its broad expression in derivatives of the pharyngeal mesoderm. In particular, underdeveloped lymphatic vessels on the dorsal side of the heart, which are not derived from the Isl1^{+} lineage, might be secondary to impaired heart growth probably due to Prox1 deletion in SHF-derived cardiomyocytes. This possibility should be considered in future research.

Another possibility to be considered is that other cell sources that may be marked with Isl1, such as first heart field-derived cells (Laugwitz et al., 2008) and neural crest cells (Engleka et al., 2012), may serve as the origin of Isl1-marked LECs. However, Klotz et al. have reported that these lineages did not contribute to cardiac lymphatic vessels, making this possibility unlikely (Klotz et al., 2015). In addition, the fact that TBX1, a T box-containing transcription factor regulating proliferation and differentiation of SHF derivatives, is required for cardiac lymphangiogenesis (L. Chen et al., 2010) may support our findings. Another report by Keenan et al. have demonstrated that cells derived from an Isl1-expressing progenitor lineage contribute to the endothelium of the cardinal veins (Keenan et al., 2012). Although Isl1-labeled cells were not detected in the cardinal veins in this study, the possibility that this population may partly contribute to SHF-derived LECs cannot be excluded and requires further study. Overall, the present findings identify *Isl1*-expressing progenitors as a novel potential origin of cardiac LECs, indicating lineage heterogeneity in LECs.

Recently, Chen and colleagues reported a previously undescribed vascular plexus beneath the aortic epicardium as aortic subepicardial vessels (ASVs) (H. I. Chen et al., 2014). ASVs first emerge as a single vessel around the aorta at E11.5 and expand thereafter, but mostly

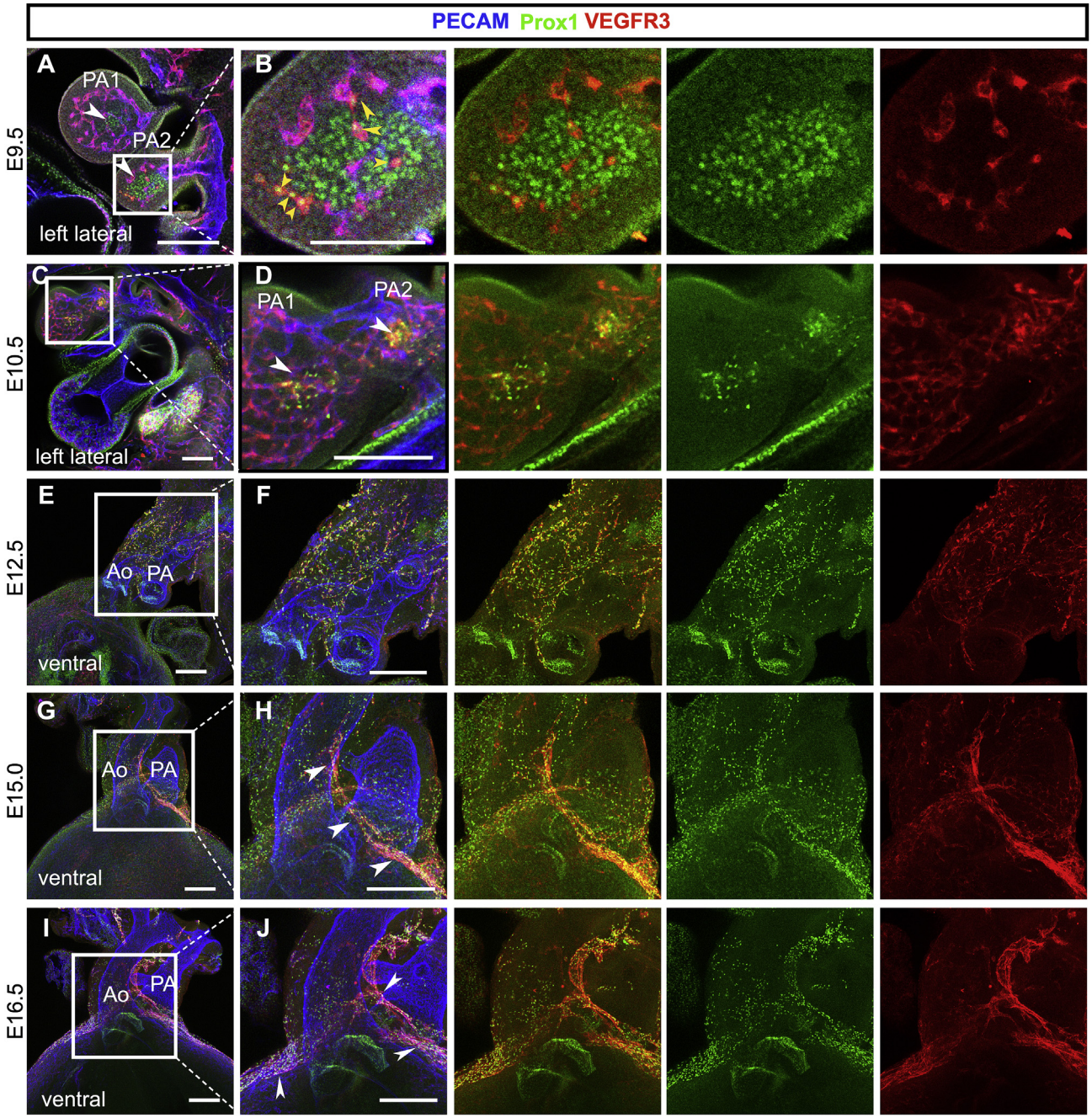

Fig. 5. Spatiotemporal dynamics of Prox1$^+$ and/or VEGFR3$^+$ cells relating to cardiac lymphatic vasculature. **(A-J)** Hearts labeled for PECAM, Prox1, and VEGFR3 on the indicated embryonic days. Boxed areas are magnified in the boxes on the right. **(A, B)** Prox1$^+$ cell clusters appear in the first and second PAs at E9.5 (white arrowheads), partially merged with PECAM and VEGFR3 (yellow arrowheads). **(C, D)** At E10.5, cell clusters in the PA express Prox1 and/or VEGFR3 (white arrowheads). **(E, F)** Prox1$^+$/VEGFR3$^+$ capillaries expand and cover the aorta at E12.5. **(G, H)** PECAM$^+$/Prox1$^+$/VEGFR3$^+$ thick cardiac lymphatics are recognized on the ventral side of the aorta at E15.0 (white arrowheads). **(I, J)** Prox1$^+$ cells around the outflow tract are remodeled and formed mature cardiac lymphatics at E16.5 (white arrowheads). PA1 and 2, first and second pharyngeal arch; Ao, aorta; PA, pulmonary artery. Scale bars, 50 μm **(A)**, 25 μm **(B)**, 100 μm **(C-J).**

disappear by E17.5. ASVs contain erythrocytes and connect to the aortic endothelium, supposing them to be blood vessels. On the other hand, a subset of early ASV endothelial cells is reported to express Prox1 and VEGFR3, with LYVE1$^+$ vessels appearing at E16.5 (H. I. Chen et al., 2014). Thus, the VEGFR3$^+$ and/or Prox1$^+$ networks surrounding the outflow tract described in this study are likely to overlap with ASVs, which may provide a base for both coronary and lymphatic vessels. Aberrant LYVE1-negative microvasculature formed by eGFP$^+$/PECAM$^+$ cells appeared in this region of *Tie2-Cre;Prox1$^{fl/fl}$* mice may reflect an altered coronary microvessel phenotype as a consequence of failed LEC differentiation.

The apparent processes of SHF-derived lymphatic vessel development, starting with *de novo* network formation followed by lumenization and then remodeling into mature vessels, is reminiscent of vasculogenesis in blood vessel formation. Recently, Wang and colleagues reported that the endothelia in pharyngeal arches 3, 4, and 6 are derived from the SHF, as in the ventral aortae and aortic sac (Wang et al., 2017). These caudal pharyngeal arch arteries were previously shown to form via

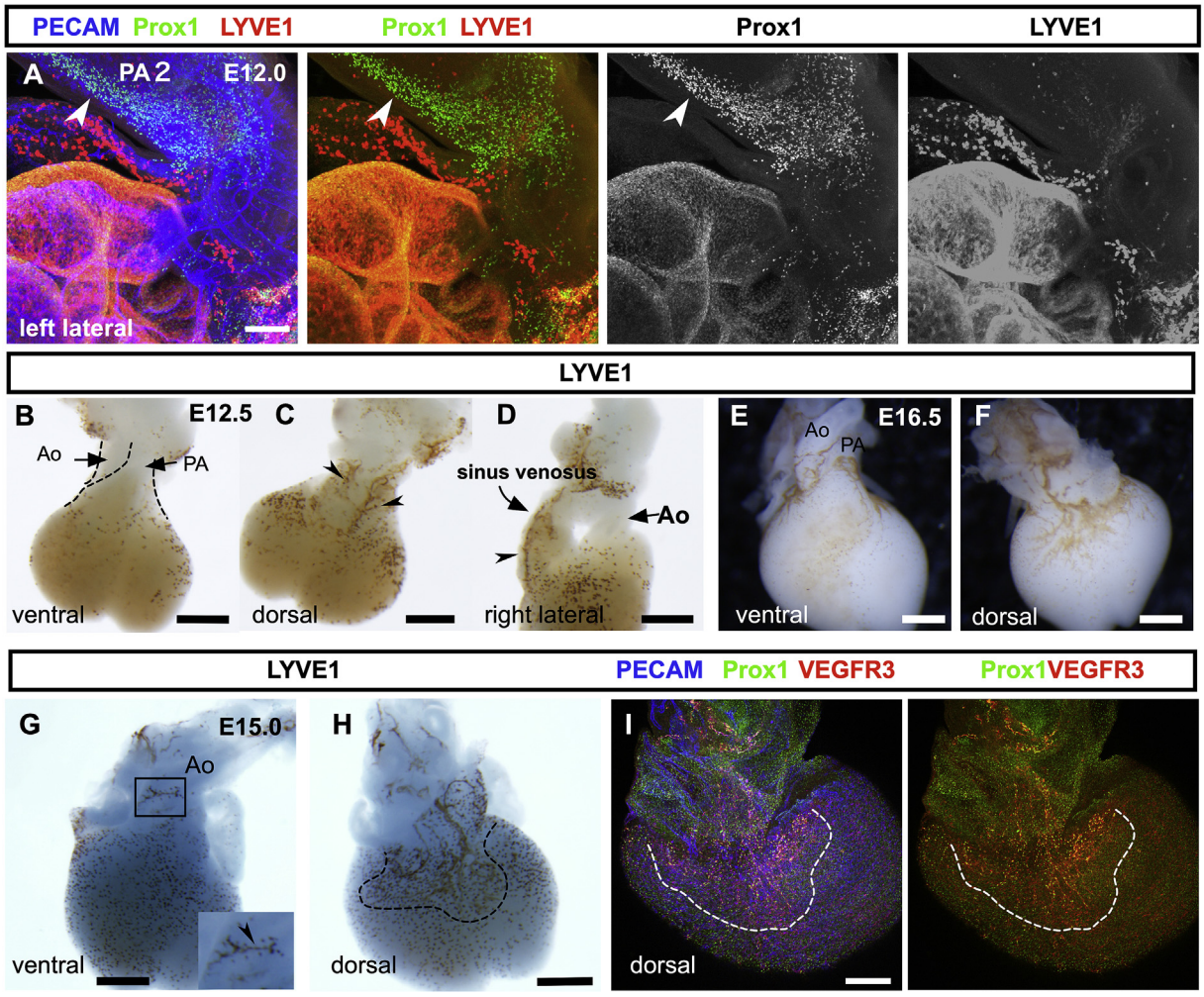

Fig. 6. LYVE1$^+$ lymphatic vessel formation in developing hearts. **(A)** Confocal images of hearts labeled for PECAM, Prox1, and LYVE1 at E12.0. Prox1$^+$ cells in the second PA (white arrowheads) do not express LYVE1. **(B-H)** Whole-mount heart immunostaining for LYVE1 on the indicated embryonic days. **(B-D)** LYVE1$^+$ lymphatic vessels are detected on the sinus venosus at E12.5 (black arrowheads) whereas no LYVE1$^+$ lymphatic vessels are on the ventral side. **(E, F)** LYVE1$^+$ lymphatic vessels spread over the dorsal and ventral sides of the ventricles at E16.5. **(G-I)** Hearts labeled for PECAM, Prox1, VEGFR3, or LYVE1 at E15.0. On the dorsal side of the hearts, PECAM$^+$/Prox1$^+$/VEGFR3$^+$/LYVE1$^+$ mature cardiac lymphatic vessels extend over the ventricular wall (black and white dotted lines). On the ventral side, LYVE1$^+$ vessels are recognized. PA2, second pharyngeal arch; Ao, aorta; PA, pulmonary artery. Scale bars, 100 μm **(A)**. 500 μm **(B-I)**.

vasculogenesis from either isolated VEGFR2$^+$/PECAM1$^+$ cells or their aggregates (Li et al., 2012). These findings, taken together, lead us to speculate that a similar mechanism may operate in both processes of SHF-derived lymphatic and blood vessel formation. In our findings, Prox1$^+$ and/or VEGFR3$^+$ cells in the Isl1$^+$ core mesoderm appear at E9.5 to E10.5 and migrate into the outflow tract. These cells may be remodeled into mature lymphatic vasculature with LYVE1 expression at E16.5. By contrast, pharyngeal arch arteries are formed much earlier at E10.5. These developmental time lag may be explained by differences in the process of migration and/or differentiation of progenitor cells to mature LECs.

In summary, we conclude that during mammalian cardiac development, *Isl1*-expressing progenitors may serve as a potential origin of cardiac LECs and contributes to lymphatic vessel formation in concert with venous- and hemogenic endothelium-derived LECs. These findings are expected to contribute to the understanding of the cellular mechanisms underlying organ-based lymphatic development. Furthermore, Klotz et al. have recently reported that lymphangiogenic response after myocardial infarction contributes to cardiac repair and function (Klotz et al., 2015). Thus, the present study may also provide insights into the developmental basis of ischemic heart disease and other lymphangiogenesis-related diseases.

4. Materials and methods

4.1. Mouse strains

The following mouse strains were used: *R26R-eYFP* (Srinivas et al., 2001), *Isl1-Cre* (Yang et al., 2006), *Tie2-Cre* (Kisanuki et al., 2001), and *Prox1*$^{fl/+}$ (Iwano et al., 2012). Their genotypes were determined via PCR using tail-tip or amnion DNA with specific primers, which are listed in Table 1. Mice were housed in an environmentally controlled room at 23 ± 2℃, with a relative humidity of 50–60% and under a 12-h light:12-h dark cycle. Embryonic stages were determined by timed mating, with the day of the plug being designated embryonic day (E) 0.5. All animal experiments were approved by the University of Tokyo and Tokyo Women's Medical University Animal Care and Use Committee, and were performed in accordance with institutional guidelines.

4.2. Immunohistochemistry, histology, confocal imaging, and quantification

For histological analysis, hearts and embryos were collected, fixed in 4% PFA for 1 h, and stored in PBS or embedded in either paraffin (Kanto Chemical, Tokyo, Japan) or OCT (Sakura Finetek, Tokyo, Japan).

Table 1
Key resources table.

Reagent or resource	Source	Identifier
Antibodies		
Rat Anti-Mouse CD31	BD Pharmingen	Cat# 553370; RRID: AB_394816
Rabbit anti-PROX1 antibody	AngioBio	Cat# 11–002; RRID: AB_10013720
Goat anti-human PROX1 antibody	R&D	Cat# AF2727; RRID: AB_2170716
Rabbit anti-LYVE1 antibody	abcam	Cat# ab14917; RPID: AB_301509
Goat anti-mouse LYVE1 antibody	R&D	Cat# AF2125 ; RPID: AB_2297188
Goat anti-mouse VEGFR3 antibody	R&D	Cat# AF743; RRID: AB_355563
Rat anti-GFP antibody	Nacalai Tesque	Cat# GF090R, RRID:AB_2314545
Rabbit anti-GFP antibody	Frontier Institute	Cat# GFP-Rb-Af2020, RRID:AB_2491093
Mouse anti-Islet1 antibody	Developmental Studies Hybridoma Bank	Cat# 40.2D6, RRID: AB_528315
Rat anti-F4/80 antibody	Invitrogen	Cat# 14-4801-82, RRID:AB_467558
Donkey Alexa Fluor 488-conjugated anti-rabbit secondary antibody	abcam	Cat# ab150073, RRID:AB_2636877
Donkey Alexa Fluor 555-conjugated anti-goat secondary antibody	abcam	Cat# ab150074, RRID:AB_2636997
Donkey Alexa Fluor 647-conjugated anti-rat secondary antibody	abcam	Cat# ab150075, RRID:AB_2752244
Bacterial and Virus Strains		
Biological Samples		
Chemicals, Peptides, and Recombinant Proteins		
Critical Commercial Assays		
Deposited Data		
Experimental Models: Cell Lines		
Experimental Models: Organisms/Strains		
B6.129X1-*Gt(ROSA)26Sor*$^{tm1(EYFP)Cos}$/J (*R26R-eYFP*)	Srinivas et al., (2001)	Cat# JAX:006148; RRID:IMSR_JAX:006148
Isl1$^{tm1(cre)Sev}$/J	Yang et al., (2006)	Cat# JAX:024242 RRID:IMSR_JAX:024242
B6.Cg-Tg(Tek-cre) 1Ywa/J (*Tie2-Cre*)	Kisanuki et al., (2001)	Cat# JAX:008863; RRID: IMSR_JAX:008863
Mouse: *Prox1+/flox*	Iwano et al., (2012)	N/A
Oligonucleotides		
Recombinant DNA		
Software and Algorithms		
ImageJ	N/A	https://imagej.nih.gov/ij/
GraphPad Prism 7	GraphPad Software Inc	https://www.graphpad.com/scientific-software/prism/
Other		

Immunostaining of 4-μm-thick paraffin or 16-μm-thick frozen sections was performed using primary antibodies against CD31 (553370, BD Pharmingen, 1:50), Prox1 (11–002, AngioBio, 1:200), Prox1 (AF2727, R&D Systems, 1:200), Lyve-1 (ab14917, Abcam, 1:250), Lyve-1 (AF2125, R&D Systems, 1:50), VEGFR-3 (AF743, R&D Systems, 1:50), GFP (GF090R, Nacalai Tesque, 1:1000), GFP (GFP-RB-AF2020, FRL, 1:200), Isl1 (40.2D6, Developmental Studies Hybridoma Bank, 1:100) and F4/80 (14-4801-82, Invitrogen, 1:500). Alexa Fluor-conjugated secondary antibodies (Abcam, 1:200) were subsequently applied. The same protocol was followed for whole-mounted hearts and embryos, with the primary and secondary antibody incubations extended to two nights. Whole-mount 3,39-diaminobenzidine (DAB) staining was performed on embryonic and postnatal hearts using the Vectastain ABC System (Vector Laboratories, Burlingame, CA, USA). Immunofluorescence imaging was conducted using a Nikon C2 confocal microscope. DAB staining was observed under a Keyence BZ-X700 microscope. All images were processed using ImageJ and Nikon NIS Elements software.

Detailed material information is in the Key Resource Table 1.

Author contributions

K.M., S.M.-T., and H.K. conceived the study and designed the experiments. K.M. performed the majority of the experiments. F.M. provided the *Prox1*$^{fl/+}$ mice. K.M., S.M.-T., K.M., and H.K. coordinated the experimental work, analyzed the data and wrote the manuscript, with contributions from all authors.

Competing financial interests

The authors declare no competing financial interests.

Acknowledgments.

We thank S. Evans (University of California, San Diego, California, USA) for the *Isl1-Cre* mice, and all the lab members for helpful discussion and encouragement. We also thank R. S. Srinivasan (Oklahoma Medical Research Foundation) for advice for manuscript. This work was supported in part by grants-in-aid for scientific research from the Ministry of Education, Culture, Sports, Science and Technology, Japan (15H02536 and 19H01048 to H. K. and r19K08308 to S.M.-T.); Platform for Dynamic Approaches to Living System from the Ministry of Education, Culture, Sports, Science and Technology, Japan; and Core Research for Evolutional Science and Technology (CREST) of the Japan Science and Technology Agency (JST), Japan (JPMJCR13W2).

Appendix A. Supplementary data

Supplementary data related to this article can be found at https://doi.org/10.1016/j.ydbio.2019.05.002.

References

Chen, H.I., Poduri, A., Numi, H., Kivela, R., Saharinen, P., Mckay, A.S., Raftrey, B., Churko, J., Tian, X., Zhou, B., Wu, J.C., Alitalo, K., Red-Horse, K., 2014. VEGF-C and aortic cardiomyocytes guide coronary artery stem development. J. Clin. Investig. 124, 4899–4914. https://doi.org/10.1172/JCI77483.

Chen, L., Mupo, A., Huynh, T., Cioffi, S., Woods, M., Jin, C., McKeehan, W., Thompson-Snipes, L., Baldini, A., Illingworth, E., 2010. Tbx1 regulates Vegfr3 and is required for lymphatic vessel development. J. Cell Biol. 189, 417–424. https://doi.org/10.1083/jcb.200912037.

Engleka, K.A., Manderfield, L.J., Brust, R.D., Li, L., Cohen, A., Dymecki, S.M., Epstein, J.A., 2012. Islet1 derivatives in the heart are of both neural crest and second heart field origin. Circ. Res. 110, 922–926. https://doi.org/10.1161/CIRCRESAHA.112.266510.

Hägerling, R., Pollmann, C., Andreas, M., Schmidt, C., Nurmi, H., Adams, R.H., Alitalo, K., Andresen, V., Schulte-Merker, S., Kiefer, F., 2013. A novel multistep mechanism for initial lymphangiogenesis in mouse embryos based on ultramicroscopy. EMBO J. 32, 629–644. https://doi.org/10.1038/emboj.2012.340.

Henri, O., Pouehe, C., Houssari, M., Galas, L., Nicol, L., Edwards-Lévy, F., Henry, J.-P., Dumesnil, A., Boukhalfa, I., Banquet, S., Schapman, D., Thuillez, C., Richard, V., Mulder, P., Brakenhielm, E., 2016. Selective stimulation of cardiac lymphangiogenesis reduces myocardial edema and fibrosis leading to improved cardiac function following myocardial infarction. Circulation 133, 1484–1497. https://doi.org/10.1161/CIRCULATIONAHA.115.020143 discussion 1497.

Huntington, G.S., McClure, C.F.W., 1910. The anatomy and development of the jugular lymph sacs in the domestic cat. Am. J. Anat. 1–181.

Iwano, T., Masuda, A., Kiyonari, H., Enomoto, H., Matsuzaki, F., 2012. Prox1 postmitotically defines dentate gyrus cells by specifying granule cell identity over CA3 pyramidal cell fate in the hippocampus. Development 139, 3051–3062. https://doi.org/10.1242/dev.080002.

Johnson, R.A., Blake, T.M., 1966. Lymphatics of the heart. Circulation 1–7.

Karkkainen, M.J., Haiko, P., Sainio, K., Partanen, J., Taipale, J., Petrova, T.V., Jeltsch, M., Jackson, D.G., Talikka, M., Rauvala, H., Betsholtz, C., Alitalo, K., 2004. Vascular endothelial growth factor C is required for sprouting of the first lymphatic vessels from embryonic veins. Nat. Immunol. 5, 74–80. https://doi.org/10.1038/ni1013.

Keenan, I.D., Rhee, H.J., Chaudhry, B., Henderson, D.J., 2012. Origin of non-cardiac endothelial cells from an Isl1+ lineage. FEBS Lett. 586, 1790–1794. https://doi.org/10.1016/j.febslet.2012.05.014.

Kisanuki, Y.Y., Hammer, R.E., Miyazaki, J.-I., Williams, S.C., Richardson, J.A., Yanagisawa, M., 2001. Tie2-Cre transgenic mice: a New model for endothelial cell-lineage analysis in vivo. Dev. Biol. 230, 230–242. https://doi.org/10.1006/dbio.2000.0106.

Klotz, L., Norman, S., Vieira, J.M., Masters, M., Rohling, M., Dubé, K.N., Bollini, S., Matsuzaki, F., Carr, C.A., Riley, P.R., 2015. Cardiac lymphatics are heterogeneous in origin and respond to injury. Nature 522, 62–67. https://doi.org/10.1038/nature14483.

Koltowska, K., Lagendijk, A.K., Pichol-Thievend, C., Fischer, J.C., François, M., Ober, E.A., Yap, A.S., Hogan, B.M., 2015. Vegfc regulates bipotential precursor division and Prox1 expression to promote lymphatic identity in zebrafish. Cell Rep. 13, 1828–1841. https://doi.org/10.1016/j.celrep.2015.10.055.

Laugwitz, K.-L., Moretti, A., Caron, L., Nakano, A., Chien, K.R., 2008. Islet1 cardiovascular progenitors: a single source for heart lineages? Development 135, 193–205. https://doi.org/10.1242/dev.001883.

Li, P., Pashmforoush, M., Sucov, H.M., 2012. Mesodermal retinoic acid signaling regulates endothelial cell coalescence in caudal pharyngeal arch artery vasculogenesis. Dev. Biol. 361, 116–124. https://doi.org/10.1016/j.ydbio.2011.10.018.

Martinez-Corral, I., Ulvmar, M.H., Stanczuk, L., Tatin, F., Kizhatil, K., John, S.W.M., Alitalo, K., Ortega, S., Mäkinen, T., 2015. Nonvenous origin of dermal lymphatic vasculature. Circ. Res. 116, 1649–1654. https://doi.org/10.1161/CIRCRESAHA.116.306170.

Nicenboim, J., Malkinson, G., Lupo, T., Asaf, L., Sela, Y., Mayseless, O., Gibbs-Bar, L., Senderovich, N., Hashimshony, T., Shin, M., Jerafi-Vider, A., Avraham-Davidi, I., Krupalnik, V., Hofi, R., Almog, G., Astin, J.W., Golani, O., Ben-Dor, S., Crosier, P.S., Herzog, W., Lawson, N.D., Hanna, J.H., Yanai, I., Yaniv, K., 2015. Lymphatic vessels arise from specialized angioblasts within a venous niche. Nature 522, 56–61. https://doi.org/10.1038/nature14425.

Ny, A., Koch, M., Schneider, M., Neven, E., Tong, R.T., Maity, S., Fischer, C., Plaisance, S., Lambrechts, D., Héligon, C., Terclavers, S., Ciesiolka, M., Kälin, R., Man, W.Y., Senn, I., Wyns, S., Lupu, F., Brändli, A., Vleminckx, K., Collen, D., Dewerchin, M., Conway, E.M., Moons, L., Jain, R.K., Carmeliet, P., 2005. A genetic Xenopus laevis tadpole model to study lymphangiogenesis. Nat. Med. https://doi.org/10.1038/nm1285.

Oliver, G., Alitalo, K., 2005. The lymphatic vasculature: recent progress and paradigms. Annu. Rev. Cell Dev. Biol. 21, 457–483. https://doi.org/10.1146/annurev.cellbio.21.012704.132338.

Risebro, C.A., Searles, R.G., Melville, A.A.D., Ehler, E., Jina, N., Shah, S., Pallas, J., Hubank, M., Dillard, M., Harvey, N.L., Schwartz, R.J., Chien, K.R., Oliver, G., Riley, P.R., 2009. Prox1 maintains muscle structure and growth in the developing heart. Development 136, 495–505. https://doi.org/10.1242/dev.030007.

Sabin, F.R., 1902. On the origin of the lymphatic system from the veins and the development of the lymph hearts and thoracic duct in the pig. Am. J. Anat. 1–23.

Schneider, M., Othman-Hassan, K., Christ, B., Wilting, J., 1999. Lymphangioblasts in the avian wing bud. Dev. Dynam. 216, 311–319. https://doi.org/10.1002/(SICI)1097-0177(199912)216, 4/5<311::AID-DVDY1>3.0.CO;2-M.

Shore, L.R., 1929. The lymphatic drainage of the human heart. J. Anat. 1–23.

Srinivas, S., Watanabe, T., Lin, C.S., William, C.M., Tanabe, Y., Jessell, T.M., Costantini, F., 2001. Cre reporter strains produced by targeted insertion of EYFP and ECFP into the ROSA26 locus. BMC Dev. Biol. 1, 4. https://doi.org/10.1186/1471-213X-1-4.

Srinivasan, R.S., Dillard, M.E., Lagutin, O.V., Lin, F.-J., Tsai, S., Tsai, M.-J., Samokhvalov, I.M., Oliver, G., 2007. Lineage tracing demonstrates the venous origin of the mammalian lymphatic vasculature. Genes Dev. 21, 2422–2432. https://doi.org/10.1101/gad.1588407.

Stanczuk, L., Martinez-Corral, I., Ulvmar, M.H., Zhang, Y., Laviña, B., Fruttiger, M., Adams, R.H., Saur, D., Betsholtz, C., Ortega, S., Alitalo, K., Graupera, M., Mäkinen, T., 2015. cKit lineage hemogenic endothelium-derived cells contribute to mesenteric lymphatic vessels. Cell Rep. https://doi.org/10.1016/j.celrep.2015.02.026.

Wang, X., Chen, D., Chen, K., Jubran, A., Ramirez, A., Astrof, S., 2017. Endothelium in the pharyngeal arches 3, 4 and 6 is derived from the second heart field. Dev. Biol. 421, 108–117. https://doi.org/10.1016/j.ydbio.2016.12.010.

Wigle, J.T., Oliver, G., 1999. Prox1 function is required for the development of the murine lymphatic system. Cell 98, 769–778. https://doi.org/10.1016/S0092-8674(00)81511-1.

Wilting, J., Aref, Y., Huang, R., Tomarev, S.I., Schweigerer, L., Christ, B., Valasek, P., Papoutsi, M., 2006. Dual origin of avian lymphatics. Dev. Biol. 292, 165–173. https://doi.org/10.1016/j.ydbio.2005.12.043.

Yang, L., Cai, C.-L., Lin, L., Qyang, Y., Chung, C., Monteiro, R.M., Mummery, C.L., Fishman, G.I., Cogen, A., Evans, S., 2006. Isl1Cre reveals a common Bmp pathway in heart and limb development. Development 133, 1575–1585. https://doi.org/10.1242/dev.02322.

Yang, Y., García-Verdugo, J.M., Soriano-Navarro, M., Srinivasan, R.S., Scallan, J.P, Singh, M.K., Epstein, J.A., Oliver, G., 2012. Lymphatic endothelial progenitors bud from the cardinal vein and intersomitic vessels in mammalian embryos. Blood 120, 2340–2348. https://doi.org/10.1182/blood-2012-05-428607.